Retraction

Retracted: Polypyrrole/Magnetic/Tea Waste Composites for PO_4^{3-} Ions Removal: Adsorption-Desorption, Kinetics, and Thermodynamics Studies

Adsorption Science and Technology

This article has been retracted by Hindawi following an investigation undertaken by the publisher [1]. This investigation has uncovered evidence of one or more of the following indicators of systematic manipulation of the publication process:

(1) Discrepancies in scope

(2) Discrepancies in the description of the research reported

(3) Discrepancies between the availability of data and the research described

(4) Inappropriate citations

(5) Incoherent, meaningless and/or irrelevant content included in the article

(6) Peer-review manipulation

The presence of these indicators undermines our confidence in the integrity of the article's content and we cannot, therefore, vouch for its reliability. Please note that this notice is intended solely to alert readers that the content of this article is unreliable. We have not investigated whether authors were aware of or involved in the systematic manipulation of the publication process.

Wiley and Hindawi regrets that the usual quality checks did not identify these issues before publication and have since put additional measures in place to safeguard research integrity.

We wish to credit our own Research Integrity and Research Publishing teams and anonymous and named external researchers and research integrity experts for contributing to this investigation.

The corresponding author, as the representative of all authors, has been given the opportunity to register their agreement or disagreement to this retraction. We have kept a record of any response received.

References

[1] F. Saleem, H. N. Bhatti, A. Khan et al., "Polypyrrole/Magnetic/Tea Waste Composites for PO_4^{3-} Ions Removal: Adsorption-Desorption, Kinetics, and Thermodynamics Studies," *Adsorption Science & Technology*, vol. 2022, Article ID 4071162, 11 pages, 2022.

Research Article

Polypyrrole/Magnetic/Tea Waste Composites for PO$_4^{3-}$ Ions Removal: Adsorption-Desorption, Kinetics, and Thermodynamics Studies

Fatima Saleem,[1] **Haq Nawaz Bhatti,**[1] **Amina Khan,**[1] **Lamia Ben Farhat,**[2,3] **Zainab Mufarreh Elqahtani,**[4] **Norah Alwadai,**[4] **and Munawar Iqbal** [5]

[1]*Department of Chemistry, University of Agriculture, Faisalabad, Pakistan*
[2]*Department of Chemistry, College of Sciences, King Khalid University, P.O. Box 9004, Abha, Saudi Arabia*
[3]*Laboratoire des matériaux et de l'environnement pour le développement durable LR18ES10, 9 Avenue Dr. Zoheir Sai, 1006 Tunis, Tunisia*
[4]*Department of Physics, College of Sciences, Princess Nourah bint Abdulrahman University, P.O. Box 84428, Riyadh 11671, Saudi Arabia*
[5]*Department of Chemistry, Division of Science and Technology, University of Education, Lahore, Pakistan*

Correspondence should be addressed to Munawar Iqbal; bosalvee@yahoo.com

The polypyrrole (PPY/TW) and magnetic (MG/TW) composite with tea waste (TW) was prepared and used as an adsorbent for PO$_4^{3-}$ ions removal from aqueous media. The composite were characterized with SEM and FTIR techniques. Batch study was conducted to investigate the effect of different reaction parameters on the adsorption of PO$_4^{3-}$ ions. The native TW, PPY/TW, and MG/TW showed the PO$_4^{3-}$ ions removal of 7.2, 7.3, and 7.9 (mg/g), respectively, using 0.05 g adsorbent dose and 10 mg/L initial concentration of PO$_4^{3-}$ ions at pH of 6, 10, and 3, respectively, and equilibrium was reached in 90 min. Kinetics and isotherm models were employed on the PO$_4^{3-}$ ions adsorption data and PO$_4^{3-}$ ions adsorption followed the pseudo-second order kinetics, intraparticle diffusion, and Langmuir isotherm models. Thermodynamics analysis reveals an exothermic process and spontaneous adsorption of PO$_4^{3-}$ ions on the composites. Results revealed that the magnetic and polypyrrole composites with tea waste have auspicious potential as an adsorbent and this class of the composites can be utilized for the removal of PO$_4^{3-}$ ions from the effluents.

1. Introduction

In view of alarming environmental pollution situation worldwide [1, 2], the phosphorus is a one of major issues, which is commonly present in water reservoirs and involves variety of complex processes mainly eutrophication and nutrient enrichment. It is widely used in industries and agricultural sectors [3]. Food industries produces beverages and products that are potent source of phosphorus; however, only 16% of it is absorbed by the human body from their diet. The fertilizers use in agricultural sector led to the increase load of phosphorus in water reservoirs by runoff through farmlands, agricultural soils, and animal manures. The quantity of phosphorus

higher than 0.02 mg/L is harmful because higher amount causes production of algal blooms which results in eutrophication [3–5]. So, it is important to maintain the quantity of phosphorus below its threshold amount.

Different approaches are in practice to remove the phosphorus along with other pollutants from wastes, and among these approaches, adsorption is suitable and highly efficient technique because of its simplicity in operational design and adsorbent recycling abilities [6–9]. Adsorption, in accordance with wastewater treatment, is accommodation of pollutant on the surface of a solid adsorbent. The pollutant that adheres to the adsorbent is called adsorbate, and so the solid material is referred as adsorbent. The rate of attachment of

pollutants on the solid surface is affected or controlled by different factors such as pH, particle size of solid adsorbent, contact time, temperature, and concentration of particular pollutant. In accordance with several advantages, biomasses proved their remarkable abilities as adsorbents to remove phosphorous from water [10–13].

These biosorbents can be algal, fungal, and bacterial biomasses and waste materials (industrial, agricultural, and domestic). The biomasses possess several functional groups, i.e., carboxyl and hydroxyl (anionic) amine groups (cationic), which help them to adsorb different anionic/cationic species through different interactions such as ion exchange, chelation, and electrostatic interactions. The waste materials from domestic, agricultural, and industrial units attracted much interest because of cost effectiveness and freely available, is a one good choice, and can be utilize them for the treatment of wastewater [14–16]. Tea waste is a renewable source, green, and sustainable adsorbent for phosphorus removal from the polluted water to manage the waste through waste. Tea waste have different biological molecules (lignin, cellulose, carbohydrates, phenolic, aromatic carboxylate, phenolic-hydroxyl, and phenolic-oxyls) which are responsible for the adsorption of adsorbate. However, limited binding sites on the surface is one drawback these materials and the efficiency of adsorbents can be increased by modifications in biomasses, which leads to the enhanced adsorption capacity of the native adsorbent [17]. Previous studies revealed that when the biomass is coupled with other functional moieties, the adsorption capacities were enhanced many folds. During modification, the physicochemical properties of the composite materials are enhanced, which can adsorb the pollutant more effectively versus native/ unmodified adsorbents [18–23].

The polypyrene and magnetic composites with tea waste biomass were prepared in this study, and same were employed for the removal of PO_4^{3-} ions from aqueous media: The adsorption was studied as a function of various process variable along with desorption of PO_4^{3-} ions from the adsorbent. The equilibrium, kinetics, and thermodynamics analysis were undertaken to analyze the nature and mechanism of PO_4^{3-} ions adsorption on to the composites.

2. Material and Methods

2.1. Reagents and Chemicals.
The formaldehyde, sodium phosphate dibasic heptahydrate, H_2SO_4, HCl, NaOH $FeCl_3.6H_2O$, sodium sulfide, ammonium molybdate, and ammonia solution were of Sigma-Aldrich. The PO_4^{3-} ions stock solution was prepared from sodium phosphate dibasic heptahydrate. The 1000 mg/L of phosphate ions stock solution was prepared, and then, it was further diluted to different concentrations in distilled water.

2.2. Preparation of Adsorbents.
Tea waste (TW) was collected from tea stall in university cafeteria, UAF, FSD, Pak. The collected TW was washed with distilled water. Then, it was treated with 5 mL formaldehyde (HCOH) and 100 mL sulfuric acid (H_2SO_4) for 48 h at 120 rpm, dried in an oven, ground, and sieved through 300 μm sieve (OCT-4527-01). Magnetic composite of TW (MG/TW) was prepared by the co-precipitation

method. Initially, 5 g biomass and 22.5 g of $FeCl_3.6H_2O$ were added in a beaker, and the beaker was kept at 60 °C with stirring on hot plate. Then, ammonia was added dropwise into the solution. Ammonia was added until the basic pH (9-11) was achieved. Black powder of magnetic composite was filtered and dried. For pyrrole composite of TW (PPY/TW), 3 g of TW was taken into a 500 mL beaker and was soaked into the pyrrole solution (0.2 M) overnight. The next day, the beaker was put onto the magnetic stirrer, and 100 mL of $FeCl_3.6H_2O$ (0.3 M) was added into it dropwise. After stirring, the black precipitates appeared at the bottom of beaker was collected and dried in oven at 60 °C.

2.3. Characterization.
FTIR analysis was done in the range of 650-4000 cm^{-1} for Native TW, PPY/TW, and MG/TW using FTIR Spectrophotometer to appraise the functional groups on the surface of the composites. The SEM analysis was employed to evaluate the morphology of the prepared biocomposites.

2.4. Adsorption Study.
The adsorption was designed to study the effect of different operating parameters, i.e., initial concentration of PO_4^{3-} ions, adsorbent dose, pH, contact time, and temperature. To investigate the effect of one parameter, all the other parameters were kept constant [24]. In this research work, the range of parameters were 0.05-0.3 g adsorbent dose, 3-10 pH, 3-15 mg/L initial concentration of PO_4^{3-} ions, 5-120 min contact time, and 27-62 °C. The PO_4^{3-} ions contaminated water (50 mL) was taken in a conical flask and was mixed and stirred at a constant speed of 120 rpm in the orbital shaker. The initial and equilibrium concentration of PO_4^{3-} ions was determined by spectrophotometer (UV-2800, USA) at 715 nm. Equatiom (1) is used to determine the PO_4^{3-} ions removal efficiency:

$$q_e = \frac{(C_i - C_e) \times V}{W}. \tag{1}$$

where C_i, q_e, C_e, W, and V are the initial concentration, adsorption efficiency, equilibrium concentration, composite dose, and solution volume, respectively.

2.5. PO_4^{3-} Ions Analysis.
For the detection of residual concentration of PO_4^{3-} ions, 0.5 mL of ammonium molybdate ($(NH_4)_2MoO_4$) and 3 mL of 0.25 N sulfuric acid (H_2SO_4) were added in the test tube. Then, 3 mL sample/filtrate (PO_4^{3-} ions solution) was transferred to a test tube, and 1 mL of 0.002 M of sodium sulfide ($Na_2S.9H_2O$) was added, and let it rest for 20 min to develop color. The initial and equilibrium concentrations of PO_4^{3-} ions were determined by Spectrophotometer (UV-2800, USA) at 715 nm.

2.6. Desorption Study.
Desorption experiments were designed to investigate the stability and reusability of adsorbents. The capability of any adsorbent to desorb suggests the restoration of adsorbent. Reagents were used like NaOH and HCl for desorption of the PO_4^{3-} ions from three adsorbents. Desorption efficiencies are calculated using the following equation:

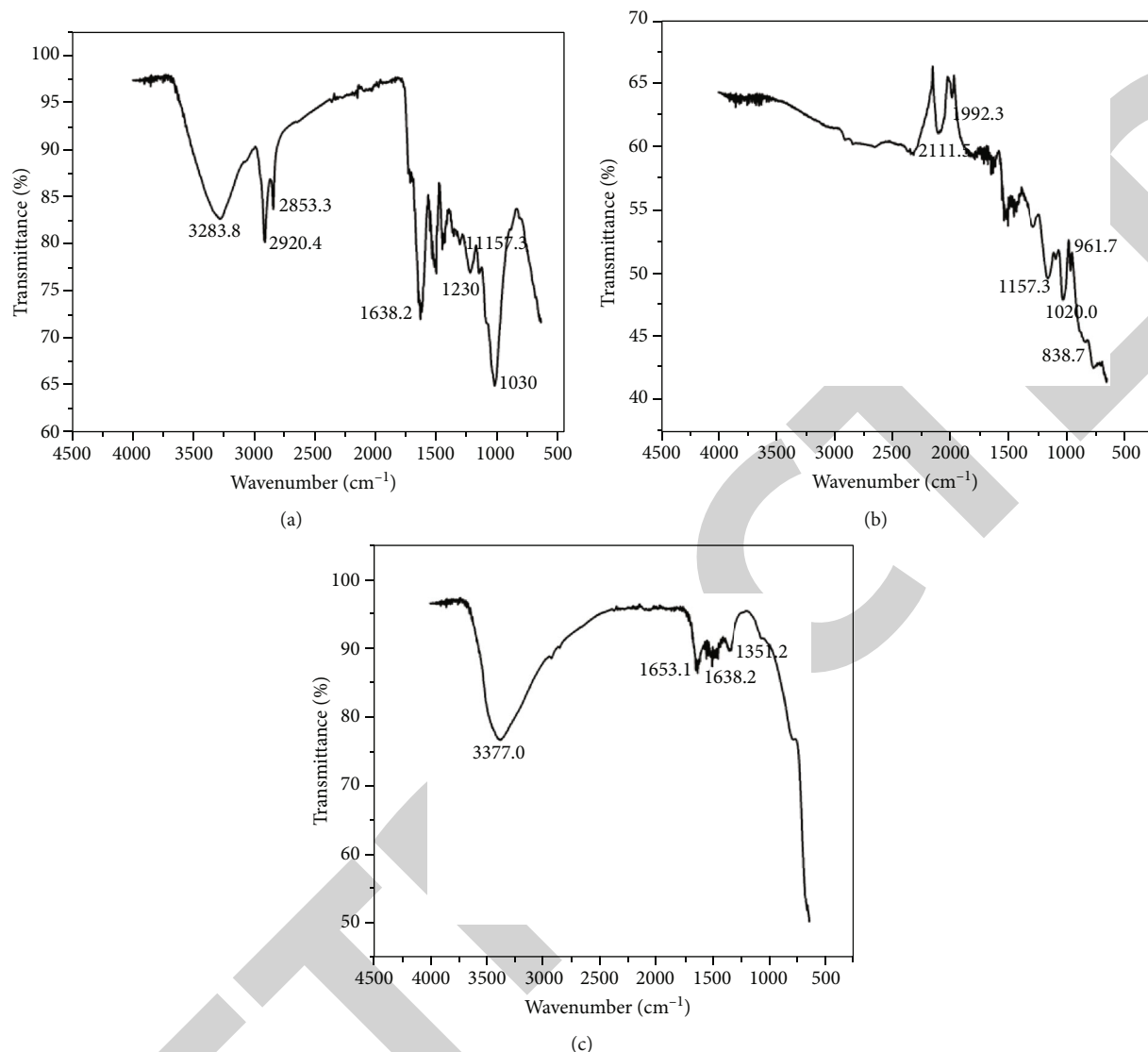$$Desorption\,(\%) = \frac{C_d - V_d}{q_e \times w}, \tag{2}$$

(a)

(b)

(c)

FIGURE 1: FTIR analysis (a) TW, (b) PPY/TW adsorbent, and (c) MG/TW adsorbent.

where $C_d, V_d, w,$ and q_e are the concentration of PO_4^{3-} ions, volume of the solution, and mass of the composite and is the amount of PO_4^{3-} ions adsorbed, respectively.

3. Results and Discussion

3.1. Characteristics of the Adsorbents. FTIR spectrum of native TW (Figure 1) showed a broad peak at 3283 cm^{-1} which is due to the presence of bonded hydroxyl groups at the surface of the native TW. Peaks in the region of 2900-2700 cm^{-1} showed the stretching of C-H bond of alkane, which are part of the complex structure of biomass. The band at 1638 cm^{-1} is due to carboxyl group stretching (-COOH). The peaks below 1190 cm^{-1} to 1130 cm^{-1} showed secondary amine and from 1090-1020 cm^{-1} peaks showed the stretching of primary amine. The FTIR spectrum of PPY/TW (Figure 1) showed the presence of several peaks in 950-1225 cm^{-1} which confirmed in-plane bending of the aromatic C-H bond. As the

structure of polypyrrole has ring structure, so these peaks are due to C-H bond in the ring of polypyrrole. The peaks in 1650-2000 cm^{-1} range appeared due to the aromatic structure. A peak in 2100-2140 cm^{-1} confirmed the presence of C≡C terminal alkyne monosubstituted. The broad peak at 3377 cm^{-1} in the FTIR spectrum of MG/TW (Figure 1) confirmed the presence of hydroxy group, H-bonded OH stretch. Alkenyl C=C stretch was observed in the peak range of 1620-1680 cm^{-1}. The peak at 1351 cm^{-1} showed that the carboxylate functional group is present in the structure of magnetic composites. The surface morphology of the native TW, PPY/TW, and MG/TW is evident from the SEM images (Figure 2). The more surface area the more will be the adsorption efficiency of the adsorbent. The SEM of native TW showed a highly porous and rough surface. The pores will contribute to the surface area of the adsorbent which can favor effective interaction of PO_4^{3-} ions with the active sites. SEM analysis of PPY/TW showed that the highly rough surface and SEM image of
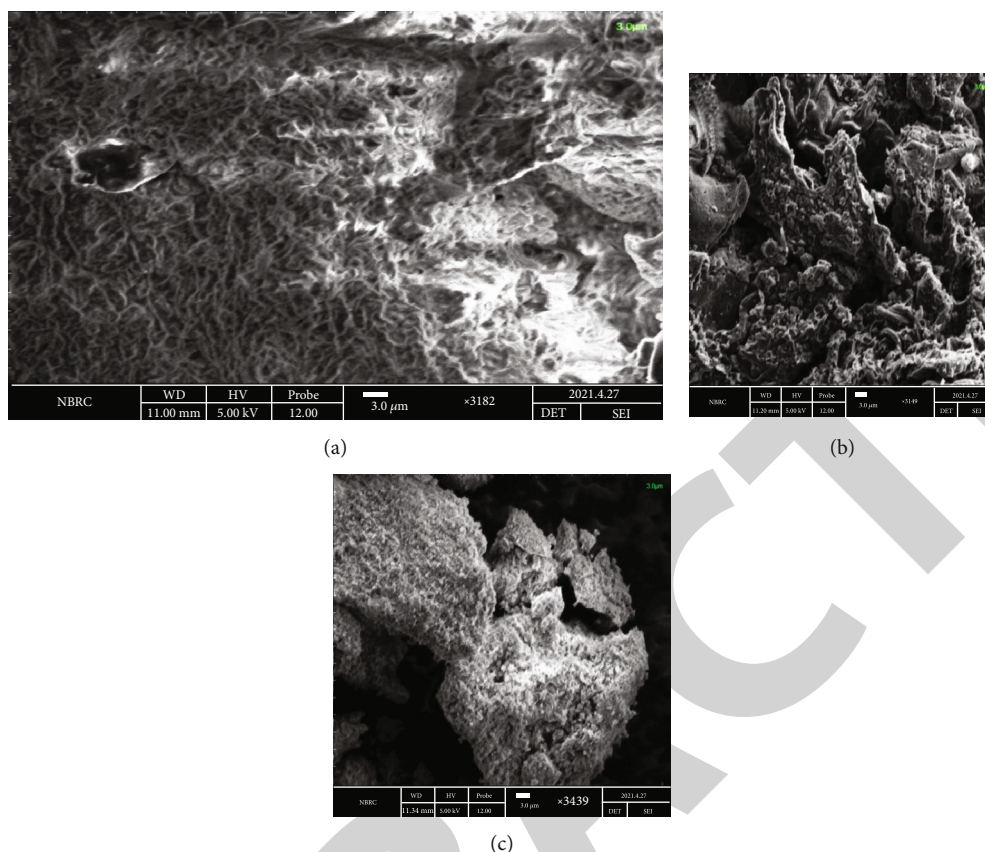
(a)

(b)

(c)

Figure 2: Surface analysis, (a) TW, (b) PPY/TW, and (c) MG/TW adsorbents.

MG/TW showed that particles are in dispersed form and are of different shapes. The MG/TW showed the mean particle size of 21.872 μm.

3.2. pH$_{pzc}$ (Point Zero Charge) Analysis. Point zero charge depict the charge on the surface of the biomass. If the pH of the point of zero charge is lower than optimum pH, then the biomass will possess a negative charge, and if pH of point zero charge is higher than the optimum pH, then the biomass have positive charge. As evident from the data (Figure 3), the pH of point zero charge (pH$_{pzc}$ 6.5) is higher than the optimum pH (6) of TW; hence, it was found that there is positive charge on biomass surface which is in accordance with the adsorption of PO$_4^{3-}$ ions. As phosphates being negatively charged will adsorb favorably on positively charged biomass.

The biosorption capacities of 50, 64.6, and 52.5 (%) were achieved for TW, MG/TW, and PPY/TW composite at pH 6, 3, and 10, respectively (Figure 4). For native tea waste, the adsorption capacity was achieved at pH 6 because in pH range 5-7, phosphorus exist in the form of H$_2$PO$_4^-$ and HPO$_4^{-2}$ and the surface of the adsorbent is positively charged due to protonation [25]. The PO$_4^{3-}$ ions adsorbed on the surface through ion exchange and electrostatic attraction. Pyrrole composites showed 5.25 mg/g removal capacity at pH 10. This may be due to the presence of another component on the surface of adsorbent where highly alkaline pH increases adsorption capacity for PO$_4^{3-}$ ions on the adsorbent surface because of
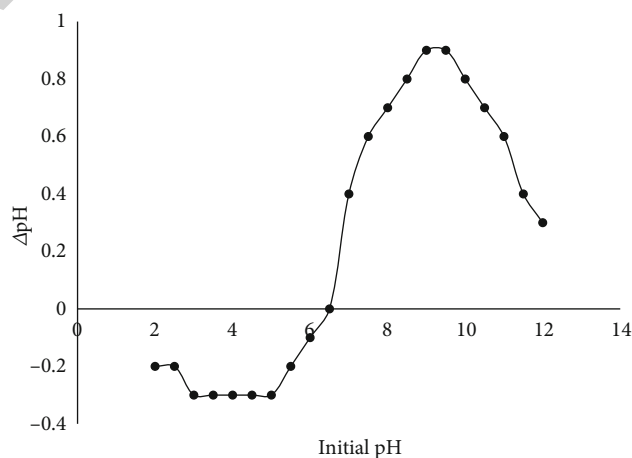
Figure 3: Point of zero charge analysis.

metal ions present on biomass surface [26]. Hence, higher pH than 10 did not favor the adsorption process because addition of alkali reduces the activity of the adsorbent. The alkaline media may block the active sites and preclude them from the efficient adsorption [27]. The basicity results in repulsion of negatively charged ions, i.e., OH$^-$ and phosphate ion. At pH 3, the surface of magnetic composites is positively charged due to protonation and adsorbed phosphate ions as H$_3$POH$_4$.

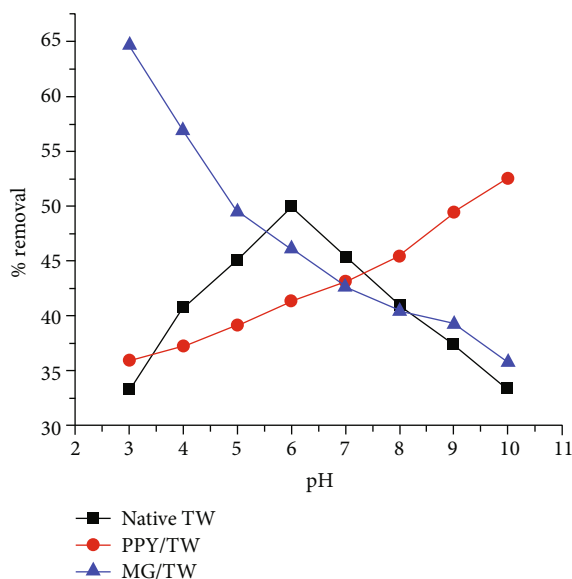FIGURE 4: . pH effect on adsorption of PO_4^{3-} ions.

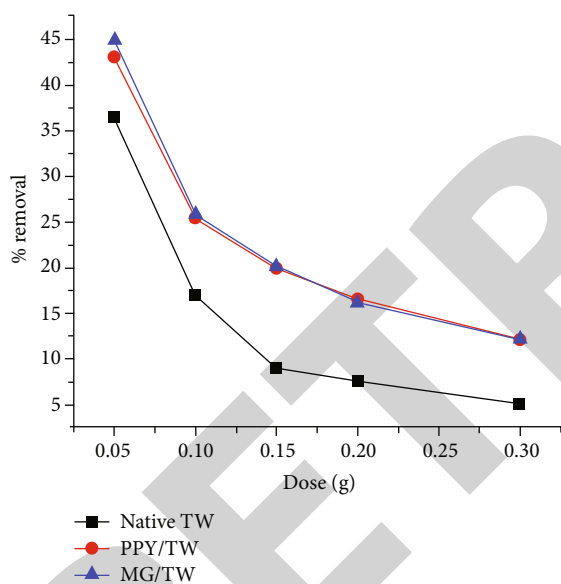FIGURE 6: Effect of contact time on PO_4^{3-} ions adsorption.

FIGURE 5: Effect of adsorbent dose on PO_4^{3-} ions adsorption.

3.3. Composite Dose Effect on PO_4^{3-} Ions Adsorption. The amount of dose determines the adsorption capacity of biomass for adsorbate molecules. Dose effect was studied for tea waste and its composites in the range of 0.05, 0.1, 0.15, 0.2, and 0.3 g by keeping all the other parameters constant at optimum pH. The optimum dose for the adsorption of PO_4^{3-} ions was determined 0.05 g/50 mL solution for native TW, PPY/TW, and MG/TW composites. Native TW, PPY/TW, and MG/TW showed percentage removal of 36, 43, and 44 (%), respectively. The dosage amount higher than 0.05 g depicted a decrease in adsorption capacity of the composites, which is due to the agglomeration of adsorbent which cover the available active sites. At higher dose, equilibrium is established, and all the active sites became saturated, and after getting this point, the
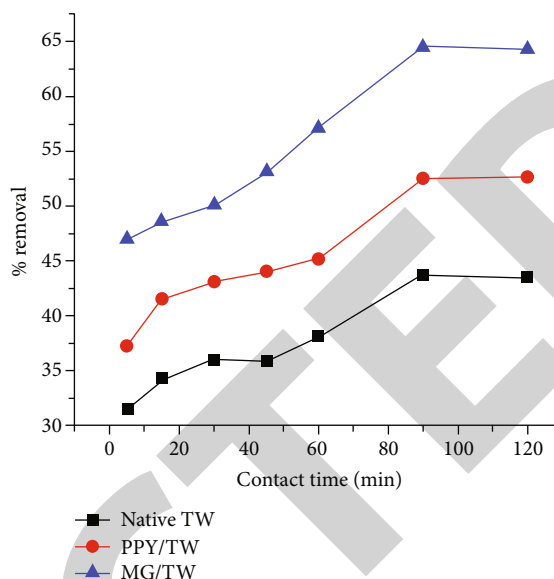
PO_4^{3-} ions started to release from the adsorbent back to the solution which decreases the removal efficiency (Figure 5).

3.4. Contact Time Effect on PO_4^{3-} Ions Adsorption. It was evident that contact time of 90 min showed the removal effectiveness of 43.79, 52.54, and 64.63 (%) for native TW, PPY/TW, and MG/TW, respectively (Figure 6). After 90 min, no further change in efficiency was noted. At the start, the adsorption efficiency was increased with contact time because the active sites on adsorbent were available for PO_4^{3-} ions and adsorption rate was fast. At equilibrium, all the active sites became saturated with adsorbate, and no further adsorption occurred because of the unavailability of active sites [28].

3.5. Initial Concentration Effect in PO_4^{3-} Ions Adsorption. To optimize the sorbate initial concentration, experiments were also conducted an optimized pH, contact time, and composite dose. Initial concentration was varied in 3-15 mg/L with 0.05 g dose of adsorbent for 90 min of contact time. The response showed a maximum removal efficiency of 43.79, 52.54, and 64.63 (%) for native TW, PPY/TW, and MG/TW, respectively, at initial concentration of 10 mg/L (Figure 7). It is evident from the data that with increase in initial concentration of PO_4^{3-} ions and removal efficiency did not increase due to saturation of active sites on adsorbents and unavailability of favorable sites for remaining PO_4^{3-} ions at higher concentration [28].

3.6. Temperature Effect on PO_4^{3-} Ions Adsorption. Figure 8 showed the adsorption capacity of native TW, PPY/TW, and MG/TW composites for the adsorption of PO_4^{3-} ions as a function of temperatures (300.15-335.15 K) at optimized conditions. The decrease in removal capacity was observed because of the instability of adsorbents at higher temperatures, and this can deteriorate the structure of the adsorbents, which is in line with previous reports [29]; a decrease in adsorption capacity was observed at higher temperature, and the same was observed in the current study; the adsorption of PO_4^{3-}
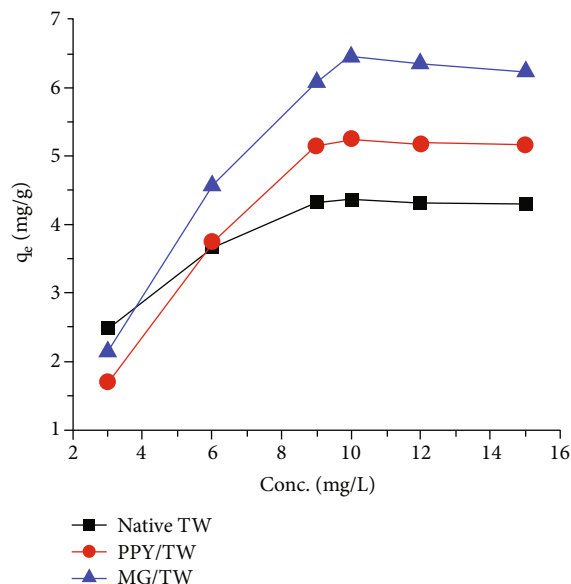
FIGURE 7: Effect of initial conc. of phosphorus on PO_4^{3-} ions adsorption.
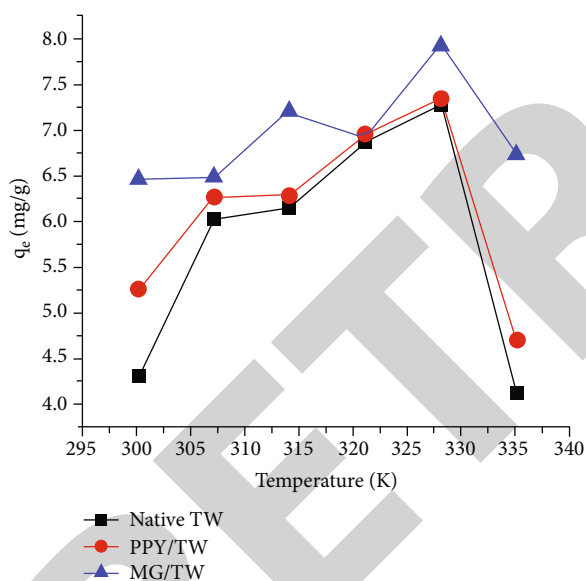

FIGURE 8: Effect of temperature on PO_4^{3-} ions adsorption.

ions was declined at higher temperature. The effect of adsorption temperature is different in the case of different adsorbents. The zirconium-modified zeolite amended with sediment revealed an increase in adsorption of phosphate at higher temperatures [30].

3.7. Kinetics Studies. The adsorption kinetics enables to analyze the rate of adsorption process and mechanism of mass transfer from liquid phase to solid adsorbent. Different kinetic models have been utilized to appraise the PO_4^{3-} ions adsorption rate. In adsorption of PO_4^{3-} ions, three models were used including pseudo-first-order (PFO), pseudo-second-order (PSO) and intraparticle diffusion models [31–33]. The PFO explains the liquid-solid adsorption system and describes the

relation between the quantity of sorbate adsorbed and time required for the same [34]. Equation (4) shows the straight line equation for the PSO.

$$\log (q_e - q_m) = \log q_e - K_1 \cdot \left(\frac{t}{2.303}\right), \quad (3)$$

Where $\log(q_e - q_m)$ is at y-axis, $\log(qe)$ is at x-axis, $K_1/2.303$ is slope ($K_1 = rate\,constant$ (L/min)), and $\log(q_e)$ is intercept. q_e is the adsorption capacity at a specific time, and q_m is the maximum adsorption capacity. The PSO describes the adsorption of adsorbate on the surface of sorbent as function of the square of active sites of the adsorbent [34]. Equation (5) shows the relation of PSO.

$$\frac{t}{q_t} = \frac{1}{K_2 qe^2} + \frac{t}{q_e}, \quad (4)$$

Where $1/K_2qe^2$ is intercept and $1/qe$ is the slope. K_2 (g/mg/min) represents the second-order kinetic rate constant, q_e (mg/g) is the maximum adsorption capacity at time t, and q_m (mg/g) is the maximum adsorption capacity at equilibrium. For the value of coefficient of determination, R^2 for the PSO obtained was 0.9916, 0.9212, and 0.9916 for native TW, PPY/TW, and MG/TW. Hence, the PO_4^{3-} ions adsorption followed the PSO.

Generally, there are different steps of the liquid-solid adsorption process. Mass transfer occurs in 4 steps: formation of layer of sorbate on the solid (external diffusion), diffusion of sorbate molecules in the pores of adsorbent (internal diffusion), transfer of sorbate to the active sites in the adsorbent, and development of interactions (adsorption, precipitation, and complexation) between sorbate molecules and macropores and micropores of the adsorbent [35]. Mechanism of adsorption can involve one step or multiple steps. As batch study involving high stirring during adsorption can undergo diffusion of film and intraparticle diffusion or sometimes both [34]. Intraparticle diffusion describes the relationship between uptake efficiency and $t^{1/2}$. The intraparticle diffusion relation is depicted in the following equation:

$$q_t = K_{pi} \cdot t^{1/2} + C_i, \quad (5)$$

where K_{pi} (mg/g min$^{1/2}$) is the slope and known as the rate constant, C_i is the intercept and q_t is the adsorption capacity at given time. The graph between $t^{1/2}$ and adsorption capacity shows whether the adsorption is intraparticle only or both. The R^2 values are above 0.90 for three adsorbents; it showed that the intraparticle diffusion of PO_4^{3-} ions adsorption occur for native TW, PPY/TW, and MG/TW composites (Table 1).

3.8. Equilibrium Studies. Isotherms are basically related to the homogeneity and heterogeneity of adsorbents and enables to finds the possible interactions between sorbate molecules and sorbent. Isotherm plots relate adsorption capacity, q_e, to the concentration of adsorbate at equilibrium [36]. These isotherms provide an overall understanding of mechanism pathways and design of adsorption systems. The following

TABLE 1: Kinetic parameters for the adsorption of PO_4^{3-} ions on the native and composite adsorbents.

Kinetic models	Parameters	Native TW	PPY/TW	MG/TW
Pseudo-first-order	R^2	0.5736	0.5988	0.6757
	K (min^{-1})	0.02	0.031	0.030
	Qe (cal.) (mg/g)	1.8	2.70	3.33
	Qe (Exp.) (mg/g)	4.3	5.2	6.4
Pseudo-second-order	R^2	0.9916	0.9212	0.9916
	K (min^{-1})	0.034	0.00043	0.02
	Qe (cal.) (mg/g)	4.53	77.5	6.75
	Qe (Exp.) (mg/g)	4.3	5.2	6.4
Intraparticle diffusion model	R^2	0.9553	0.9801	0.976
	K_{pi}	0.144	0.175	0.22
	C_i	2.80	3.355	3.988

TABLE 2: Equilibrium parameters for the adsorption of PO_4^{3-} ions on the native and composite adsorbents.

Models	Parameter	Native TW	PPY/TW	MG/TW
Langmuir model	B	0.297	0.1479	0.137
	R_L	0.313	0.403	0.42
	R^2	0.9981	0.9023	0.962
	Q_m (cal.) (mg/g)	4.55	6.76	7.29
	Q_m (exp.) (mg/g)	4.37	5.25	6.46
Freundlich	N	5.13	1.92	2.40
	K_f	2.98	2.01	3.20
	R^2	0.9112	0.7264	0.7065
Temkin	A	106.70	3.32	7.77
	B	0.6553	1.7072	1.7034
	R^2	0.9178	0.7747	0.7606
Huskin-Jura	A	5.62	1.98	5.57
	B	1.173	0.89	0.861
	R^2	0.7082	0.631	0.4794
Dubinin-Radushkevich	β (mol^{2}KJ^{-2})	8×10^{-8}	6×10^{-7}	3×10^{-7}
	R^2	0.9553	0.9801	0.9764
	Q_m (cal.) (mg/g)	4.29	5.82	6.91
	q_m (Exp.) (mg/g)	4.37	5.25	6.46
	E (KJ/mole)	0.625	0.833	1.67

isotherms were applied to the adsorption data of PO_4^{3-} ions on to the composites.

3.8.1. Langmuir Isotherm. Langmuir isotherm is based on the postulation that the adsorption of adsorbate molecules on the surface of the sorbent forms monolayer which means that one molecule attaches at the particular active site. Energy of the adsorption process remains constant, and none of the molecules moves across the surface of the sorbent, and it represents that adsorption is homogenous [36]. Langmuir model is represented in the following equation:

$$\frac{C_e}{q_e} = \frac{1}{q_m b} + \frac{C_e}{q_m}, \qquad (6)$$

where C_e/q_e is y-axis, C_e (mg/L) is the concentration of adsorbate at time t, $1/q_m$ is slope, q_m is maximum adsorption capacity at equilibrium state, $1/q_m b$ is intercept, and b is the Langmuir constant also represented as K_L. Essential features of adsorption can be explained by a dimensionless constant of Langmuir constant called separation factor R_L (Equation (8)):

$$R_L = \frac{1}{1 + bC_o}, \qquad (7)$$

where C_o is initial concentration of adsorbate (mg/L). R_L value indicates the adsorption is favorable or not. If its value range between 0 and 1, it means adsorption if favorable, and if greater than 1, then adsorption in unfavorable and adsorption is irreversible when the value is 0. The values of R^2 indicate

TABLE 3: Thermodynamic parameters for the adsorption of PO_4^{3-} ions on the native and composite adsorbents.

Temperature (K)	300.15	307.15	314.15	321.15	328.15	335.15
Native TW						
ΔG (kJ/mole)	0.7	− 1.06	− 1.21	− 2.10	− 2.69	0.98
ΔH (kJ/mole)	6.66					
ΔS (J/mole.K)	0.024					
PPY/TW						
ΔG (kJ/mole)	− 1.50	− 1.56	− 2.48	− 2.16	− 3.66	− 2.01
ΔH (kJ/mole)	− 31.24					
ΔS (J/mole.K)	− 0.096					
MG/TW						
ΔG (kJ/mole)	− 1.50	− 1.57	− 2.48	− 2.16	− 3.66	− 2.01
ΔH (kJ/mole)	9.27					
ΔS (J/mole.K)	0.036					

that adsorption data of PO_4^{3-} ions followed Langmuir model and the adsorption of PO_4^{3-} ions on the native TW, PPY/TW, and MG/TW is monolayer adsorption.

3.8.2. Freundlich Isotherm. The adsorption that occurs at the heterogeneous surfaces is explained by Freundlich isotherm [37]. The linear form of Freundlich isotherm is depicted in the following equation:

$$\log q_e = \log K_F + \frac{1}{n(\log C_e)}, \tag{8}$$

where K_F, $1/n$, C_e, and q_e are the adsorption capacity, intensity, PO_4^{3-} ions concentration at equilibrium, and adsorption capacity at equilibrium, respectively. Adsorption intensity indicates the distribution of the energy and the heterogeneity of the adsorption. The following are the results obtained for adsorption of PO_4^{3-} ions on adsorbents by applying Freundlich model. Adsorption data of PO_4^{3-} ions of native TW followed Freundlich isotherm model (Table 2).

3.8.3. Temkin Isotherm. The Linear form of Temkin isotherm model is shown in the following equation [36]:

$$Q_e = BlnA + BlnC_e, \tag{9}$$

where $B = RT/b$ and A = equilibrium binding constant. In the straight-line equation, B is the slope, and $BlnA$ is the intercept. The Temkin model explains the distribution of binding energies over active sites and revealed that heat of adsorption decreases with the increase of coverage of sites. We can calculate the values of the slope, intercept, and R^2 by plotting graph between lnC_e and q_e. Value of R^2 showed that adsorption of PO_4^{3-} ions on native TW followed Temkin isotherm model, while PPY/TW and MG/TW did not follow the Temkin model.

3.8.4. Harkin-Jura Isotherm. Multilayer adsorption on the adsorbent and heterogeneous pore distribution is explained by Harkin-Jura isotherm [37]. Linear form of this model is shown in the following equation:

$$\frac{1}{qe^2} = \frac{B}{A} - \frac{1}{A} \log C_e, \tag{10}$$

where $1/qe^2$ (y-axis), $logC_e$ (x-axis), $1/A$ is the slope, and B/A is the intercept. The values of A and B can be calculated by plotting a graph between $logC_e$ and $1/qe^2$. The following is the graphical representation of the model for PO_4^{3-} ions the adsorption on the TW, PPY/TW, and MG/TW composites. None of the adsorption data fitted well to the Harkin-Jura isotherm model.

3.8.5. Dubinin-Radushkevich Isotherm. This model gives us an estimation about the free energy of porosity of adsorbent and heterogeneous surface of adsorbent [38]. Dubinin-Radushkevich isotherm model is represented in the following equation:

$$\ln q_e = \ln q_m - \beta \varepsilon^2, \tag{11}$$

where β is the slope and lnq_m is intercept. ε can be calculated using Equation (13), and the values of E can be estimated using the following equation:

$$\varepsilon = RTln\left(1 + \frac{1}{C_e}\right), \tag{12}$$

$$E = \frac{1}{2\beta^{1/2}}, \tag{13}$$

where ϵ is Polanyi potential, β is Dubinin-Radushkevich constant, R is gas constant (8.31 $Jmol^{-1}k^{-1}$), T is absolute temperature, and E is mean adsorption energy. Values of R^2 are noted 0.9553, 0.9801, and 0.9764 for Native TW, PPY/TW, and MG/TW, respectively. All the adsorbents followed the Dubinin-Radushkevich isotherm which showed that this process is temperature dependent. The values of all equilibrium parameters are given in Table 2.

3.9. Thermodynamics Studies. Thermodynamics of adsorption gives us the estimation that how change in enthalpy (ΔH) and entropy (ΔS) determines the free energy content
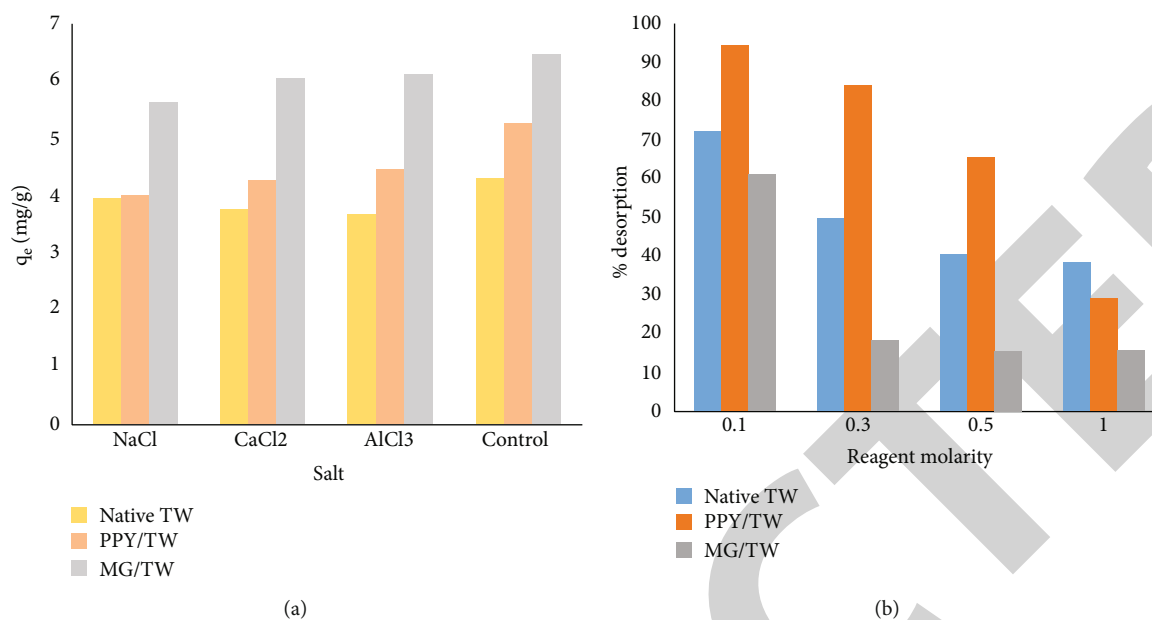
(a)

(b)

FIGURE 9: (a) Salt effect on the adsorption of PO_4^{3-} ions and (b) Desorption study of PO_4^{3-} ions.

TABLE 4: Adsorption efficiency comparison of composites for different inorganic ions.

S. no	Adsorbent	Adsorbate	Removal efficiency	References
1	Graphene oxide and Fe_3O_4 composite	NO_3^- and PO_4^{3-} ions	89 and 93 (%)	[5]
2	Zeolite/geopolymer composite	PO_4^{3-} and NH_4^+ ions	206 and 140 (mg/g)	[41]
3	Mango stone biocomposite	PO_4^{3-} ions	95 mg/g	[3]
4	g-C_3N_4 and acid-activated montmorillonite composite	PO_4^{3-} and Pb(II) ions	5.06 and 182.7 (mg/g)	[42]

(ΔG) of the adsorption process at constant temperature and pressure [39]. According to thermodynamics, the PO_4^{3-} ions will spontaneously adsorb on the surface of adsorbent if the change in free energy will be negative. Equations (14) and (15) utilize for the thermodynamics analysis:

$$\Delta G = \Delta H - T\Delta S, \tag{14}$$

$$\ln K_d = -\frac{\Delta H}{RT} + \frac{\Delta S}{R}, \tag{15}$$

where K_d is equilibrium rate constant, ΔH is change in enthalpy change, ΔS is entropy change, R is general gas constant (8.314 J/mole.K), and T is absolute temperature. The values of ΔH and ΔS were calculated from the plot of $\ln K_d$ versus 1/T. Negative values of ΔG for native TW, PPY/TW, and MG/TW indicated that the adsorption of PO_4^{3-} ions is exothermic and spontaneous. Change in entropy ΔS was positive for native TW and MG/TW. Table 3 showed the values of the thermodynamic parameters for PO_4^{3-} ions adsorption on to native TW, PPY/TW, and MG/TW.

3.10. Effect of Interfering Ions on Adsorption. Wastewater streams contain with different type of salts and their presence effect the adsorption capabilities of the adsorbents. Adsorption of PO_4^{3-} ions was affected in the presence of the monovalent, divalent, and trivalent salts. The NaCl, $CaCl_2$, and $AlCl_3.6H_2O$

salts (0.025 g) were taken in 50 mL of 10 mg/L phosphate solution with 0.05 g adsorbent at optimized pH values and were run in an orbital shaker for 90 min at 120 rpm. The presence of salts decreases the adsorption capacity. The effect of $AlCl_3.6H_2O$ on MG/TW was negligible, but NaCl and $CaCl_2$ have significantly reduced the removal efficiency. It was because of blockage of active sites with the salt ions rather than the PO_4^{3-} ions. It was clear from the data analysis that monovalent ions decreased the sorption capacity more than divalent and trivalent ions for all the adsorbents. The order of reducing removal efficiency can be represented as $Na^+ > Ca^{2+} > Al^{3+}$. The removal efficiency was reduced from 43 to 39 (%), 52 to 40 (%), and 64 to 56 (%) in the presence of monovalent ions for native TW, PPY/TW, and MG/TW, respectively (Figure 9).

3.11. Desorption Study. Desorption experiments were designed to investigate the stability and reusability of adsorbents. The capability of any adsorbent to desorb suggests the recycling of the adsorbent, which made the adsorbent cost-effective. The desorption study of PO_4^{3-} ions from native TW, MG/TW, and PPY/TW was studied in a 0.5-0.25 g range using reagent molarity (0.1-1.0 N). Native TW and MG/TW showed maximum adsorption with 0.1 N NaOH and minimum at 1 N NaOH solution, while PPY/TW showed maximum desorption in 0.1 N HCl and minimum with 1 N HCl solution (Figure 9). Percentage desorption obtained was 72.66, 61.03, and 94.43 (%) for native TW, MG/TW, and PPY/TW composites,

respectively, using NaOH and HCl (0.1 N) solution. These findings revealed that the PPY/TW and MG/TW has promising efficiency for the adsorption of PO_4^{3-} ions and their subsequent recovery. Hence, these composite can be employed for the adsorption of PO_4^{3-} ions from the effluents since adsorption has various advantages versus other conventional techniques [40]. Previous findings also revealed that the composites offer higher adsorption efficacies versus their native counterpart for the inorganic ions removal from the effluents (Table 4), which could be employed for the removal of inorganic ions from the wastewater to avoid their negative impact.

4. Conclusions

This research work illustrates the applicability of tea waste composite for the treatment of PO_4^{3-} ions. The adsorption of PO_4^{3-} ions was maximum for native TW, PPY/TW, and MG/TW at pH of 6, 10, and 3. Other optimum parameters were 0.05 g composite dose, 90 min contact time, and 10 mg/L initial PO_4^{3-} ion concentration at 55 °C. The PSO and intra-particle diffusion models fitted well to the PO_4^{3-} ions adsorption onto composites. Equilibrium isotherm fitted best for Langmuir isotherm that confirms the homogenous monolayer adsorption of PO_4^{3-} ions. The Dubinin-Radushkevich isotherm confirms that the adsorption of PO_4^{3-} ions onto the three adsorbents is temperature dependent. Thermodynamics proved exothermic and spontaneous nature of the adsorption. PO_4^{3-} ions adsorption is affected in the presence of salts, and monovalent salts lower the uptake of PO_4^{3-} ions more than the divalent and trivalent salts. Native TW and magnetic composites can be regenerated using NaOH as eluting agent. Hence, the composites have promising adsorption potential, which can be applied for the sequestration of PO_4^{3-} ions from the effluents and also extendable for other inorganic ions commonly present in the effluents.

Data Availability

Data will be made available on request.

Conflicts of Interest

The authors declare that they have no conflicts of interest.

Acknowledgments

References

[1] M. Abbas, "Experimental investigation of activated carbon prepared from apricot stones material (ASM) adsorbent for removal of malachite green (MG) from aqueous solution," *Adsorption Science & Technology*, vol. 38, no. 1-2, pp. 24–45, 2020.

[2] M. Abbas, Z. Harrache, and M. Trari, "Removal of gentian violet in aqueous solution by activated carbon equilibrium, kinetics, and thermodynamic study," *Adsorption Science & Technology*, vol. 37, no. 7-8, pp. 566–589, 2019.

[3] H. N. Bhatti, J. Hayat, M. Iqbal, S. Noreen, and S. Nawaz, "Bio-composite application for the phosphate ions removal in aqueous medium," *Journal of Materials Research and Technology*, vol. 7, no. 3, pp. 300–307, 2018.

[4] F. Hussain, S. Z. Shah, H. Ahmad et al., "Microalgae an eco-friendly and sustainable wastewater treatment option: biomass application in biofuel and bio-fertilizer production," *A review, Renewable and Sustainable Energy Reviews*, vol. 137, article 110603, 2021.

[5] S. Perveen, R. Nadeem, M. Iqbal et al., "Graphene oxide and Fe3O4 composite synthesis, characterization and adsorption efficiency evaluation for NO3⁻ and PO43⁻ ions in aqueous medium," *Journal of Molecular Liquids*, vol. 339, article 116746, 2021.

[6] A. M. Awwad and M. A. Amer, "Adsorption of Pb(II), cd(II), and cu(II) ions onto SiO_2/kaolinite/Fe_2O_3 composites: modeling and thermodynamics properties," *Chemistry International*, vol. 8, pp. 95–100, 2022.

[7] L. Zafar, A. Khan, U. Kamran, S.-J. Park, and H. N. Bhatti, "_Eucalyptus (camaldulensis)_ bark-based composites for efficient Basic Blue 41 dye biosorption from aqueous stream: kinetics, isothermal, and thermodynamic studies," *Surfaces and Interfaces*, vol. 31, article 101897, 2022.

[8] G. Jalal, N. Abbas, F. Deeba, T. Butt, S. Jilal, and S. Sarfraz, "Efficient removal of dyes in textile effluents using aluminum-based coagulants," *Chemistry International*, vol. 7, no. 3, pp. 197–207, 2021.

[9] K. Djehaf, A. Z. Bouyakoub, R. Ouhib et al., "Textile wastewater in Tlemcen (Western Algeria): impact, treatment by combined process," *Chemistry International*, vol. 3, pp. 414–419, 2017.

[10] U. Kamran and S.-J. Park, "MnO2-decorated biochar composites of coconut shell and rice husk: an efficient lithium ions adsorption-desorption performance in aqueous media," *Chemosphere*, vol. 260, article 127500, 2020.

[11] K. M. Elsherif, A. El-Dali, A. A. Alkarewi, and A. Mabrok, "Adsorption of crystal violet dye onto olive leaves powder: equilibrium and kinetic studies," *Chemistry International*, vol. 7, pp. 79–89, 2021.

[12] A. M. Alkherraz, A. K. Ali, and K. M. Elsherif, "Removal of Pb (II), Zn (II), Cu (II) and Cd (II) from aqueous solutions by adsorption onto olive branches activated carbon: equilibrium and thermodynamic studies," *Chemistry International*, vol. 6, pp. 11–20, 2020.

[13] E. C. Jennifer and O. P. Ifedi, "Modification of natural bentonite clay using cetyl trimetyl-ammonium bromide and its adsorption capability on some petrochemical wastes," *Chemistry International*, vol. 5, pp. 269–273, 2019.

[14] N. Abbas, M. T. Butt, M. M. Ahmad, F. Deeba, and N. Hussain, "Phytoremediation potential of Typha latifolia and water hyacinth for removal of heavy metals from industrial wastewater," *Chemistry International*, vol. 7, pp. 103–111, 2021.

[15] F. Minas, B. S. Chandravanshi, and S. Leta, "Chemical precipitation method for chromium removal and its recovery from

tannery wastewater in Ethiopia," *Chemistry International*, vol. 3, pp. 392–405, 2017.

[16] S. Jafarinejad, "Activated sludge combined with powdered activated carbon (PACT process) for the petroleum industry wastewater treatment: a review," *Chemistry International*, vol. 3, pp. 368–377, 2017.

[17] B. Debnath, D. Haldar, and M. K. Purkait, "Environmental remediation by tea waste and its derivative products: a review on present status and technological advancements," *Chemosphere*, vol. 300, article 134480, 2022.

[18] M. Maqbool, S. Sadaf, H. N. Bhatti et al., "Sodium alginate and polypyrrole composites with algal dead biomass for the adsorption of Congo red dye: kinetics, thermodynamics and desorption studies," *Surfaces Interfaces*, vol. 25, article 101183, 2021.

[19] S. U. Khan, M. Sultan, A. Islam et al., "Sodium alginate blended membrane with polyurethane: desalination performance and antimicrobial activity evaluation," *International Journal of Biological Macromolecules*, vol. 182, pp. 72–81, 2021.

[20] M. M. Khan, A. Khan, H. N. Bhatti et al., "Composite of polypyrrole with sugarcane bagasse cellulosic biomass and adsorption efficiency for 2,4-dicholrophonxy acetic acid in column mode," *Journal of Materials Research and Technology*, vol. 15, pp. 2016–2025, 2021.

[21] Q.-u.-a. Khalid, A. Khan, H. N. Bhatti et al., "Cellulosic biomass biocomposites with polyaniline, polypyrrole and sodium alginate: insecticide adsorption-desorption, equilibrium and kinetics studies," *Arabian Journal of Chemistry*, vol. 14, no. 7, article 103227, 2021.

[22] U. Kamran and S.-J. Park, "Hybrid biochar supported transition metal doped MnO2 composites: efficient contenders for lithium adsorption and recovery from aqueous solutions," *Desalination*, vol. 522, article 115387, 2022.

[23] U. Kamran, H. N. Bhatti, S. Noreen, M. A. Tahir, and S.-J. Park, "Chemically modified sugarcane bagasse-based biocomposites for efficient removal of acid red 1 dye: kinetics, isotherms, thermodynamics, and desorption studies," *Chemosphere*, vol. 291, article 132796, 2022.

[24] I. H. Dakhil, G. F. Naser, and A. H. Ali, "Assessment of modified rice husks for removal of aniline in batch adsorption process: optimization and isotherm study, journal of," *Ecological Engineering*, vol. 22, pp. 179–189, 2021.

[25] J. Goscianska, M. Ptaszkowska-Koniarz, M. Frankowski, M. Franus, R. Panek, and W. Franus, "Removal of phosphate from water by lanthanum-modified zeolites obtained from fly ash," *Journal of Colloid and Interface Science*, vol. 513, pp. 72–81, 2018.

[26] O. Bastin, F. Janssens, J. Dufey, and A. Peeters, "Phosphorus removal by a synthetic iron oxide-gypsum compound," *Ecological Engineering*, vol. 12, no. 3-4, pp. 339–351, 1999.

[27] V. Shettigondahalli Ekanthalu, S. Narra, J. Sprafke, and M. Nelles, "Influence of acids and alkali as additives on hydrothermally treating sewage sludge: Effect on phosphorus recovery, yield, and energy value of hydrochar," *Processes*, vol. 9, no. 4, p. 618, 2021.

[28] P. R. Rout, P. Bhunia, and R. R. Dash, "Modeling isotherms, kinetics and understanding the mechanism of phosphate adsorption onto a solid waste: ground burnt patties," *Chemical Engineering*, vol. 2, no. 3, pp. 1331–1342, 2014.

[29] J. Ye, X. Cong, P. Zhang et al., "Operational parameter impact and back propagation artificial neural network modeling for phosphate adsorption onto acid-activated neutralized red mud," *Journal of Molecular Liquids*, vol. 216, pp. 35–41, 2016.

[30] M. Yang, J. Lin, Y. Zhan, and H. Zhang, "Adsorption of phosphate from water on lake sediments amended with zirconium-modified zeolites in batch mode," *Ecological Engineering*, vol. 71, pp. 223–233, 2014.

[31] S. Lagergren, "Zur theorie der sogenannten adsorption gel Zur theorie der sogenannten adsorption gelster stoffe," *Kungliga Svenska Vetenskapsakademiens, Handlingar*, vol. 24, pp. 1–39, 1898.

[32] W. J. Weber Jr. and J. C. Morris, "Kinetics of adsorption on carbon from solution," *Journal of the Sanitary Engineering Division*, vol. 89, no. 2, pp. 1–59, 1963.

[33] Y.-S. Ho and G. McKay, "Pseudo-second order model for sorption processes," *Process Biochemistry*, vol. 34, no. 5, pp. 451–465, 1999.

[34] M. Benjelloun, Y. Miyah, G. A. Evrendilek, F. Zerrouq, and S. Lairini, "Recent advances in adsorption kinetic models: their application to dye types," *Arabian Journal of Chemistry*, vol. 14, no. 4, article 103031, 2021.

[35] J. Wang and X. Guo, "Adsorption kinetic models: physical meanings, applications, and solving methods," *Journal of Hazardous Materials*, vol. 390, article 122156, 2020.

[36] P. S. Kumar and K. Kirthika, "Equilibrium and kinetic study of adsorption of nickel from aqueous solution onto bael tree leaf powder, journal of engineering," *Science and Technology*, vol. 4, pp. 351–363, 2009.

[37] N. Ayawei, A. N. Ebelegi, and D. Wankasi, "Modelling and interpretation of adsorption isotherms," *Journal of Chemistry*, vol. 2017, Article ID 3039817, 11 pages, 2017.

[38] M. A. Al-Ghouti and D. A. Da'ana, "Guidelines for the use and interpretation of adsorption isotherm models: a review," *Journal of Hazardous Materials*, vol. 393, article 122383, 2020.

[39] R. A. Latour, "Fundamental principles of the thermodynamics and kinetics of protein adsorption to material surfaces," *Colloids and Surfaces B: Biointerfaces*, vol. 191, article 110992, 2020.

[40] U. Kamran, K. Y. Rhee, S.-Y. Lee, and S.-J. Park, "Innovative progress in graphene derivative-based composite hybrid membranes for the removal of contaminants in wastewater: a review," *Chemosphere*, vol. 306, article 135590, 2022.

[41] M. A. Salam, M. Mokhtar, S. M. Albukhari et al., "Synthesis of zeolite/geopolymer composite for enhanced sequestration of phosphate (PO_4^{3-}) and ammonium (NH_4^+) ions; equilibrium properties and realistic study," *Journal of Environmental Management*, vol. 300, article 113723, 2021.

[42] X. Wan, M. A. Khan, F. Wang et al., "Facile synthesis of protonated g-C_3N_4 and acid-activated montmorillonite composite with efficient adsorption capacity for PO_4^{3-} and Pb(II)," *Chemical Engineering Research and Design*, vol. 152, pp. 95–105, 2019.